

# A simple approach to the chaos-order contributions in nuclear spectra

A.G. Magner,<sup>\*</sup> A.I. Levon,<sup>†</sup> and S.V. Radionov<sup>‡</sup>  
*Institute for Nuclear Research, 03680 Kyiv, Ukraine*

(Dated: April, 2nd, 2018)

A simple one-parameter nearest neighbor-spacing distribution is suggested for statistical analysis of nuclear spectra and is used at the analysis of collective states in heavy nuclei. This distribution is derived within the Wigner-Dyson approach in the linear approximation for the level repulsion density of quantum states. The results are in good agreement with the two-parameter version of this distribution and Brody approach but gives the separate information concerning the Wigner and Poisson contributions.

## 1. Introduction.

Statistical analysis of quantum energy spectra for complex many-body systems such as atomic nuclei is in fruitful progress; see, e.g., one of the latest excellent review article by Gomez et al. [1] (also references therein). Different statistical methods have been proposed to obtain information on the chaoticity versus regularity in nuclear spectra. To satisfy their statistical criteria, the main idea was to use an ensemble of several nuclei with a few same given quantum numbers, such as the angular momentum and parity of the collective states. The short-range fluctuation properties in experimental spectra are analyzed usually in terms of the nearest-neighbor spacing distributions (NNSDs). For a quantitative measure of the degree of chaoticity of the many-body dynamics, the statistical probability distribution  $p(s)$  as function of spacings  $s$  between the nearest neighboring levels can be derived within the general Wigner-Dyson (WD) approach based on the level repulsion density  $g(s)$  (the units will be specified below) [1–5],

$$p(s) = g(s) \exp\left(-\int_0^s g(s') ds'\right). \quad (1)$$

For systems with definite Hamiltonians [4, 5], the order is approximately associated with the Poisson dependence of  $p(s)$  on the spacing  $s$  variable, that is obviously related to a constant  $g(s)$ , independent of  $s$ . A chaoticity can be referred, mainly, to the Wigner distribution, as clearly follows for  $g(s) \propto s$  [6].

For a further study of the order-chaos properties of nuclear systems, it might be worth to apply a simple analytical approximation to Eq. (1), keeping the link with a level repulsion density  $g(s)$  [5, 7, 8]. For analysis of the statistical properties in terms of the mixed Poisson and Wigner distributions, one can use the linear WD (LWD) approximation to the level repulsion density  $g(s)$  [7, 8]. It was the two-parameter LWD; in contrast, e.g., to the one-parameter Brody approach [3, 9]. In addition, the LWD approximation, as based on a smooth analytical (linear) function  $g(s)$  of  $s$ , can be founded properly

within the WD theory (see Refs. [5, 7, 8]). Moreover, it gives a more proper information on the separate Poisson order-like and Wigner chaos-like contributions. To reduce NNSDs to one parameter and, at the same time, keep the same quantitative individual information of their order and chaos contributions is still an attractive subject of the research.

In the present work, we derive the one-parameter probability distribution  $p_1(s)$  based on the linear approximation (LWD1) to the level repulsion density  $g(s)$  of the WD theory and compare with previously presented approaches. In Ref. [8], the two-parameter LWD2  $p_2(s)$  [7, 8] was fitted to the experimental statistical distributions of the collective energies in deformed nuclei [10–20] as well as the Brody distribution [9]. These results are in accordance with the works of Shriner et al. [21–24], see discussions in Ref. [8]. They are alternative to that for the nuclear states of single-particle nature; see, e.g., Refs. [25, 26]. The statistical properties of the nuclear collective states are discussed below using results of fitting NNSDs by the LWD1.

## 2. WD LWD approach.

The key quantity in Eq. (1) is the level repulsion density  $g(s)$ . It is convenient to consider  $s$  in units of the average  $D$  of distances between levels,  $s = S/D$ , where  $S$  is the energy spacing, i.e., the distance between the neighbor levels in usual energy units. Thus,  $D$  is locally a mean distance between neighboring levels in energy units.

For the probability distribution  $p(s)$  as function of the dimensionless variable  $s$  through the level repulsion density  $g(s)$ , one has the two normalization conditions:

$$\int_0^\infty p(s) ds = 1, \quad \int_0^\infty s p(s) ds = 1. \quad (2)$$

For the Poisson  $g(s) = 1$  and Wigner  $g(s) \propto s$  limits, from Eq. (1) one has the corresponding well known distributions, which obey Eq. (2),

$$p_P(s) = \exp(-s), \quad p_W(s) = \left(\frac{\pi s}{2}\right) \exp\left(-\frac{\pi s^2}{4}\right). \quad (3)$$

The density  $g(s)$  in fact is not a constant or simply proportional to  $s$ . The two-parameter distribution based on the linear approximation to the level repulsion den-

<sup>\*</sup> Email: magner@kinr.kiev.ua

<sup>†</sup> Email: levon@kinr.kiev.ua

<sup>‡</sup> Email: sergey.radionov@matfys.lth.se

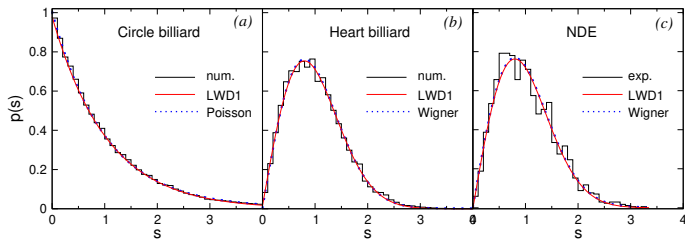


FIG. 1. NNSDs  $p(s)$  as functions of a dimensionless spacing variable  $s$  for (a) Poisson- and (b) Wigner-like numerical calculations and (c) experimental Wigner-like results (see text) by staircase lines. LWD1 NNSDs (9) are shown by solid lines. Dots present the Poisson (a) and Wigner (b,c) curves (3).

sity  $g(s)$  [7, 8], that bridges the Poisson and Wigner (3) limits, can be simplified by reducing it to one parameter.

Keeping a link with the analytical properties of the level repulsion density  $g(s)$ , it is convenient to define the probability  $p(s)$  [Eq. (1)] for a general smooth density  $g(s)$  as a polynomial of not too a large power. As shown in Refs. [7, 8], it is important to care of this density smoothness in the derivation of Eq. (1). For the simplest statistical analysis in terms of the Poisson- and Wigner-like distribution contributions, one can use the expansion of  $g(s)$  in a few powers of  $s$ , where  $a$ ,  $b$  and so on are parameters. Substituting this expansion for the linear case,

$$g(s) \approx a + bs, \quad (4)$$

into the general Wigner-Dyson formula (1), one obtains explicitly the analytically simple distribution

$$p_{\text{LWD}}(s) = (a + bs) \exp\left(-as - \frac{b}{2}s^2\right). \quad (5)$$

Taking the limits  $a \rightarrow 1$ ,  $b \rightarrow 0$  and  $a \rightarrow 0$ ,  $b \rightarrow \pi/2$  in Eq. (5), one simply arrives relatively at the standard Poisson  $g_P(s)$  and Wigner  $g_W(s)$  distributions (3). In this way, a linear approximation (4) unifies analytically these two limit cases through a smooth level repulsion density  $g(s)$ . Its parameters  $a$  and  $b$  in Eq. (4) [after their normalization by Eq. (2)] measure the probability to have separately the Poisson and Wigner distribution contributions.

As the first normalization condition in Eq. (2) obeys identically, one should care of only the second normalization condition. This requires a relation between the parameters  $a$  and  $b$  [marked by low index one in  $p_{\text{LWD}}(s)$ ]:

$$\int_0^\infty s p_1(s) ds \equiv \sqrt{\frac{\pi}{2b}} e^{w^2} \operatorname{erfc}(w) = 1, \quad (6)$$

where

$$w = a/\sqrt{2b}, \quad (7)$$

and

$$\operatorname{erfc}(w) = 1 - \operatorname{erf}(w) \equiv 1 - \frac{2}{\sqrt{\pi}} \int_0^w dx \exp(-x^2) \quad (8)$$

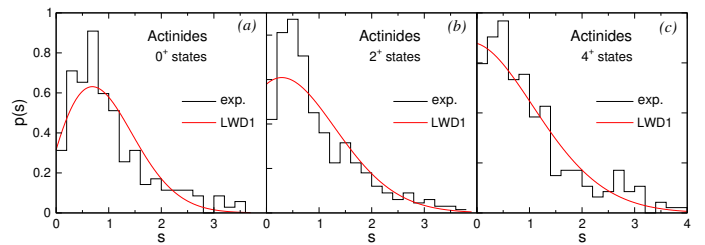


FIG. 2. The same as in Fig. 1 but for different experimental states in the actinide nuclei; (a-c): for  $0^+$ ,  $2^+$ , and  $4^+$ , respectively. The same fits by the LWD1 are shown by solid lines.

is the standard error function. Solving Eq. (6) with respect to  $b = b(w)$  and using Eq. (7) for  $a = a(w)$ , one finds

$$p_1(s) = [a(w) + b(w)s] \exp\left[-a(w)s - \frac{b(w)}{2}s^2\right], \quad (9)$$

where

$$a = \sqrt{\pi} w e^{w^2} \operatorname{erfc}(w), \quad b = \frac{\pi}{2} e^{2w^2} \operatorname{erfc}^2(w). \quad (10)$$

Thus, the probability distribution which obeys both normalization conditions (2) is given by Eq. (9), where  $a(w)$  and  $b(w)$  are functions of only one parameter  $w$  through Eq. (10). Eq. (9) with the value  $w = 0$  is the Wigner distribution ( $a = 0$ ,  $b = \pi/2$ ) and  $w = \infty$  corresponds to the Poisson distribution ( $a = 1$ ,  $b = 0$ ). Thus, the probability density (9) is a simple analytical continuation from the Poisson  $g_P(s)$  to Wigner  $g_W(s)$  limit distributions through a smooth linear level-repulsion density  $g(s)$ .

### 3. Discussions.

Fig. 1 shows the results of testing the LWD1 [Eqs. (9)] by fitting the NNSDs with a good statistics: The numerical quantum spectra in the circular (a) and heart (b) billiards, and the nuclear data ensemble [NDE, (c)]. The latter includes 1726 neutron and proton resonance energies [27]. The LWD1 is in good agreement both with numerical (a,b) and experimental NDE (c) NNSDs, as well with the corresponding Poisson (a) and Wigner (b,c) limits, see also Table I. This table presents also the least-square fitting parameters of the LWD1 to the numerical and experimental NNSDs. The sampling intervals for building the NNSD (after the unfolding procedure [8]) in Fig. 1 and others are given by  $\gamma_s = 0.1$  and  $0.2$ , respectively. They are taken from the condition of the stable smoothed NNSD values without sharp jumps between the neighbor data (see Ref. [8]). In Table I, the critical ratio

$$lRR = p_1(s_{\text{max}})/p_1(0) = (b/a) \exp[(b^2 - a^2)/2b], \quad (11)$$

where  $s_{\text{max}} = 1 - a/b$  is the value of  $s$  for the maximum of the distribution  $p_1(s)$  [Eq. (9)], describes a closeness of the distribution shape to the Wigner ( $\mathcal{R} = 0$ ) or Poisson ( $\mathcal{R} \rightarrow \infty$ ) distributions.

Experimental NNSDs for the collective states, which are excited in several actinide nuclei with different angular momenta  $I = 0^+, 2^+, 4^+$  and all fitted by the one-parameter LWD1 approximation (9), are presented in

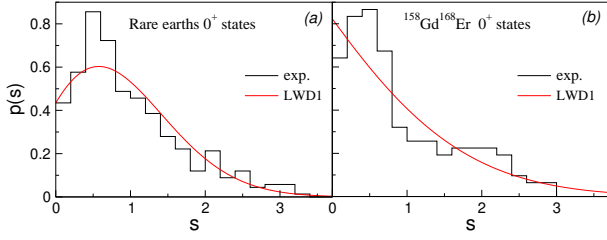


FIG. 3. The same as in Fig. 2 but for experimental states  $0^+$  in the rare earth nuclei: up to energy 3 MeV (a) and up to about 4 MeV (b). The same fits by the LWD1 are shown by solid lines.

Figure	system	$a_1$	$b_1$	$w$	$\mathcal{R}$	$\chi_1^2$	$a_2$	$b_2$	$\chi_2^2$
1a	circle	0.98	0.02	4.79	$4 \cdot 10^{11}$	0.99	0.96	0.04	1.1
b	heart	0.08	1.41	0.05	0.03	3.6	0.09	0.99	2.0
c	NDE	0.07	1.44	0.04	0.02	0.99	0.08	1.03	5.6
2a	$0^+$	0.32	0.98	0.23	0.2	11.4	0.27	1.01	9.2
b	$2^+$	0.58	0.54	0.56	1.1	11.8	0.52	0.72	10.2
c	$4^+$	0.68	0.40	0.76	2.5	9.1	0.67	0.41	8.5
3a	$0^+$	0.43	0.77	0.35	0.4	9.2	0.43	0.69	8.1
b	$0^+$	0.82	0.20	1.30	19.6	11.7	0.83	0.26	11.3
4a	$0^+$	0.35	0.91	0.26	0.3	12.0	0.38	0.80	10.5
b	$0^+_{\text{th}}$	0.49	0.68	0.42	0.6	13.1	0.45	0.91	9.7
c	$0^+_{\text{th}}$	0.72	0.33	0.89	4.03	10.5	0.68	0.54	8.7

TABLE I. Parameters  $a_i$ ,  $b_i$  and  $w$  of one- and two-parameter LWDi approximations ( $i = 1, 2$ ) [see Ref. [8] for  $i = 2$ ] for the exemplary cases and collective excited states in several nuclei. Results: Fig. 1(a) and (b) are the NNSDs given for the numerical circle and heart billiard calculations [1], (c) presents NNSDs for many experimental neutron-resonance NDE [1, 27]; Fig. 2(a-c) is for experiments with actinides; Fig. 3(a) yields experiments for rare earths at energies up to 3 MeV and (b) for  $^{158}\text{Gd}$  and  $^{168}\text{Er}$  up to 4.2 MeV; Fig. 4(a) shows experiments for the same actinides as in Fig. 2(a) (up to 3 MeV), (b) is the same but theoretical (th) results, and (c) the same as in Fig. 2(b) but up to 4 MeV. The ratio  $\mathcal{R}$  [Eq. (??)] is shown in the 6th column. The accuracies  $\chi_i^2$  of the least-square fittings (in percents) are shown in the 7th and 10th columns for the LWD1 and LWD2, respectively.

Figs. 2 and 3, see also the parameters of these fittings given in Table I.

For many rare-earth nuclei (see the row 7 in Tabl. I) the experimental  $0^+$  state energies are limited by the 3 MeV excitation [15–19]. The experimental NNSD for nuclei  $^{158}\text{Gd}$  [16] and  $^{168}\text{Er}$  [19] (see the row 8 in this table) is a special case since only for these two nuclei the measurements were carried out for larger excitation energies up to 4.2 MeV.

As seen from Table I, the results for one- and two-parameter NNSDs are close and agreed with those of the experimental data [11–14, 20]. As was pointed in Ref. [8], all spectra in the same energy interval 0–3 MeV demonstrate an intermediate structure between an order and a chaos structure with varying dominance of the Wigner to the Poisson contribution for increasing the angular momentum from  $0^+$  to  $4^+$ . With increasing

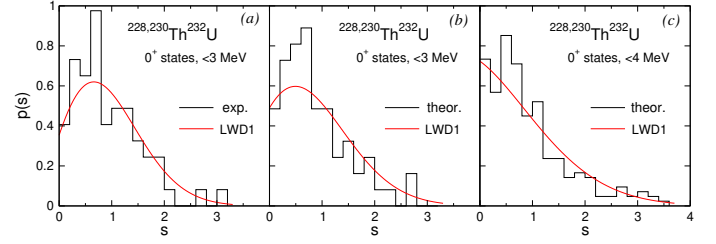


FIG. 4. Comparison of the NNSD between the experimental data (a) and the theoretical quasiparticle-phonon model results (b) in the energy interval up to 3 MeV in the  $^{228,230}\text{Th}$  and  $^{232}\text{U}$  actinide nuclei, and those (c) - up to 4 MeV. Other notations are the same as in Figs. 2.

angular momentum, one can see a shift of the NNSD to the Poisson limit in accordance with Ref. [8]. Spectra  $0^+$  in the energy interval 0–3 MeV (see Fig. 2 and Tabl. I) are intermediate between an order and a little more pronounced chaos structure, while the ordered nature is dominant for the experimental spectra in the extended energy interval about 0–4 MeV.

Fig. 4 presents the distributions for  $0^+$  states in a few actinides [8]. The experimental NNSD in the region of 0–3 MeV (a) is compared with the two theoretical distributions obtained by the quasiparticle-phonon model [28]. One of them is given in the same energy region (b) and another distribution – in the extended energy interval 0–4 MeV (c). The parameters for the distributions shown on the panels (a) and (b) are approximately the same within the error limit accuracy. This agreement between the experimental and theoretical results confirms the collective nature of the  $0^+$  states and, finally, the completeness of the level sequences. At the same time, the theoretical distribution for the energy interval 0–4 MeV [Fig. 4(c)] is shifted to the Poisson law as compared to the experimental and theoretical distributions in the interval 0–3 MeV. It is in agreement with the results obtained for the  $^{158}\text{Gd}$  and  $^{168}\text{Er}$  nuclei.

#### 4. Conclusions.

We derived the simple one-parameter NNSD approximation to the Wigner-Dyson probability distribution. It was demonstrated how it is working in solving several exemplary problems: standard circular (Poisson) and cordial (Wigner) billiards, and famous experimental neutron-resonance states in many nuclei (Fig. 1). Using this approximation we provide the statistical analysis of the nuclear collective excitations with several spins (Figs. 2 and 3):  $0^+$  in a number of the rare-earth nuclei; and  $0^+$ ,  $2^+$ , and  $4^+$ , in many actinides to show a good agreement with one-parameter LWD1, also with the two-parameter LWD2. For the linear approximation to the level repulsion density, one obtains a clear information on the quantitative measure of the Poisson order and Wigner chaos contributions in the experimental data, separately, in contrast to the heuristic Brody approach. However, as shown in Ref. [8], one finds in our calculations that the Brody formula [9] agrees largely well with the two-parameter LWD2 probability-distribution results and, therefore, with one-parameter LWD1 [Eq. (9)]. The precision of fitting the experimen-

tal data by the two-parameter LWD2 is somewhat better but the full analytical one-parameter LWD1 has the obvious advantage that the second normalization condition is identically satisfied and there is no need to check its precision.

We found the intermediate structure between the Poisson and Wigner statistical peculiarities of the experimental spectra by evaluating their separate contributions (Figs. 2 and 3). Also, one finds that the Wigner contribution dominates in the NNSD for  $0^+$  states and the Poisson contribution is larger with increasing the angular momentum. The NNSD for a smaller excitation-energy region can be described better by the Wigner distribution. The NNSD for an extended energy interval of the collective excitations, including higher energies, becomes more close to the Poisson distribution.

The experimental NNSDs are in agreement with the theoretical calculations for the same energy interval within the quasiparticle phonon model [28], that confirms the completeness of the used spectra (Fig. 4). The comparison of these results with the theoretical ones for larger energy interval supports the same conclusion

about a shift from the Wigner to the Poisson contribution dominance in the case of the collective excitations energies. As emphasized in Ref. [1], for the collective states in deformed nuclei the statistical distributions are closer to the Poisson distribution, and in other cases the situation is intermediate (see also Ref. [23]). This picture looks in agreement with our statistical results for the collective states [8].

As perspectives, it will be worth to understand the influence of the symmetry breaking phenomena on these distributions of the collective states in deformed nuclei.

#### Acknowledgements.

We are grateful to M. Spieker for providing us with experimental results before publication, also to K. Arita, S. Aberg, J. Blocki, S. Mizutori, K. Matsuyanagi, V.A. Plujko, and P. Ring for many helpful discussions. One of us (A.G.M.) is also very grateful for kind hospitality during his working visits of Physical Department of the Nagoya Institute of Technology, also the Japanese Society of Promotion of Sciences for financial support, Grant No. S-14130.

- 
- [1] J. M. G. Gomez, K. Kar, V. K. B. Kota, R. A. Molina, A. Relano, and J. Retamosa, *Phys. Rept.* **499**, 103 (2011).
- [2] C. E. Porter, *Statistical Theories of Spectra: Fluctuations* (Academy Press, New York, 1965).
- [3] T. A. Brody, J. Flores, J. B. French, P. A. Mello, A. Pandey, and S. S. M. Wong, *Rev. Mod.*, **53**, 385 (1981).
- [4] M. L. Mehta, *Random Matrices* (Academic Press, San Diego, New York, Boston, London, Sydney, Tokyo, Toronto, 1991).
- [5] S. Aberg, *Quantum Chaos* (Mathematical Physics, Lund, 2002).
- [6] E. P. Wigner, *Proc. Philos. Soc.*, **47**, 790 (1951).
- [7] J. P. Blocki and A. G. Magner, *Phys. Rev. C* **85**, 064311 (2012).
- [8] A. I. Levon, A. G. Magner, and S. V. Radionov, arXiv:1711.01848v2, (2017); in press, *Phys. Rev. C*, 2018.
- [9] T. A. Brody, *Lett. Nuovo Cimento* **7**, 482 (1973).
- [10] A. I. Levon, J. de Boer, G. Graw, R. Hertenberger, D. Hofer, J. Kvasil, A. Löscher, E. Müller-Zanotti, M. Würkner, H. Baltzer, V. Grafen, and C. Günther, *Nucl. Phys. A* **576**, 267 (1994).
- [11] A. I. Levon, G. Graw, Y. Eisermann, R. Hertenberger, J. Jolie, N. Yu. Shirikova, A. E. Stuchbery, A. V. Sushkov, P. G. Thirolf, H.-F. Wirth, N. V. Zamfir, *Phys. Rev. C* **79**, 014318 (2009).
- [12] A. I. Levon, G. Graw, R. Hertenberger, S. Pascu, P. G. Thirolf, H.-F. Wirth, P. Alexa, *Phys. Rev. C* **88**, 014310 (2013).
- [13] A. I. Levon, P. Alexa, G. Graw, R. Hertenberger, S. Pascu, P. G. Thirolf, and H.-F. Wirth, *Phys. Rev. C* **92**, 064319 (2015).
- [14] M. Spieker, D. Bucurescu, J. Endres, T. Faestermann, R. Hertenberger, S. Pascu, S. Skalacki, S. Weber, H.-F. Wirth, N.V. Zamfir, and A. Zilges, *Phys. Rev. C* **88**, 041303(R) (2013).
- [15] S. R. Leshner, A. Aprahamian, L. Trache, A. Oros-Peusquens, S. Deyliz, A. Gollwitzer, R. Hertenberger, B. D. Valnion, and G. Graw *Phys. Rev. C* **66**, 051305R (2002).
- [16] D. Bucurescu, G. Graw, R. Hertenberger, H.-F. Wirth, N. Lo Iudice, A. V. Sushkov, N. Yu. Shirikova, Y. Sun, T. Faestermann, R. Krucken, M. Mahgoub, J. Jolie, P. von Brentano, N. Braun, S. Heinze, O. Moller, D. Mucher, C. Scholl, R. F. Casten, and D. A. Meyer, *Phys. Rev. C* **73**, 064309 (2006).
- [17] D. A. Meyer, V. Wood, R. F. Casten, C. R. Fitzpatrick, G. Graw, D. Bucurescu, J. Jolie, P. von Brentano, R. Hertenberger, H.-F. Wirth, N. Braun, T. Faestermann, S. Heinze, J. L. Jerke, R. Krucken, M. Mahgoub, O. Moller, D. Mucher, and C. Scholl, *Phys. Rev. C* **74**, 044309 (2006).
- [18] L. Bettermann, S. Heinze, J. Jolie, D. Mucher, O. Moller, C. Scholl, R. F. Casten, D. Meyer, G. Graw, R. Hertenberger, H.-F. Wirth, and D. Bucurescu, *Phys. Rev. C* **80**, 044333 (2009).
- [19] A. I. Levon et al., to be published.
- [20] M. Spieker et al., private communications (2017).
- [21] T. von Egidy, H.H. Schmidt, A.N. Behkami, *Nucl. Phys. A* **481**, 189 (1988).
- [22] J. F. Shriner Jr., E. G. Bilpuch, P. M. Endt, G. E. Mitchell, *Z. Phys. A* **335**, 393 (1990).
- [23] J. F. Shriner Jr., G. E. Mitchell, T. von Egidy, *Z. Phys. A* **338**, 309 (1991).
- [24] J. F. Shriner Jr., C. A. Grossmann, and G. E. Mitchell, *Phys. Rev. C* **62**, 054305 (2004).
- [25] B. Dietz, A. Heusler, K. H. Maier, A. Richter, *Phys. Rev. Lett.*, **118**, 012501 (2017);
- [26] B. A. Brown, L. Munoz, R.A. Molina, J.M.G. Gomez, and A. Heusler, *Phys. Rev. C* **95**, 14317 (2017).
- [27] R.U. Haq, A. Pandey, O. Bohigas, *Phys. Rev. Lett.* **48** 1086 (1982).
- [28] V. G. Soloviev, *Theory of Atomic Nuclei: Quasiparticles and Phonons* (Institute of Physics, Bristol, 1992).